J. Astrophys. Astr. (2018) 39:35
https://doi.org/10.1007/s12036-018-9528-3

Color–magnitude relations in nearby galaxy clusters

MARIWAN A. RASHEED[1,2,*] and KHALID K. MOHAMMAD[1]

[1]Department of Physics, College of Science, University of Sulaimani, Sulaimani, Kurdistan Region, Iraq.
[2]Development Center for Research and Training (DCRT), University of Human Development, Sulaimani, Kurdistan Region, Iraq.
*Corresponding author. E-mail: mariwan.rasheed@univsul.edu.iq

MS received 13 February 2018; accepted 8 May 2018; published online 1 June 2018

Abstract. The rest-frame (g–r) /M_r color–magnitude relations of 12 Abell-type clusters are analyzed in the redshift range ($0.02 \lesssim z \lesssim 0.10$) and within a projected radius of 0.75 Mpc using photometric data from SDSS-DR9. We show that the color–magnitude relation parameters (slope, zero-point, and scatter) do not exhibit significant evolution within this low-redshift range. Thus, we can say that during the look-back time of $z \sim 0.1$ all red sequence galaxies evolve passively, without any star formation activity.

Keywords. Galaxies: clusters—Galaxies evolution—Galaxies: photometry.

1. Introduction

Galaxy clusters contain large populations of galaxies (of different morphologies), concentrated in a relatively small region of the sky with almost the same redshift. This makes them important astrophysical laboratories for the study of galaxy formation and evolution.

Early-type galaxies (E/S0's) are found to form a sequence in color–magnitude space, called a red sequence, in such a way that their colors become bluer towards fainter magnitudes. This so-called color–magnitude relation (CMR) was first noted, for field elliptical galaxies, by Baum (1959). In clusters, early-type galaxies show a similar correlation between colors and magnitudes (Visvanathan and Sandage 1977; Bower *et al.* 1992a,b). The dispersion of the CMR was investigated quantitatively by Bower *et al.* (1992b). By achieving precision photometry of the early-type galaxies in two nearby clusters Coma and Virgo, they observed a very small scatter about the average. This was also observed in distant clusters (Ellis *et al.* 1997; van Dokkum *et al.* 1998; Gladders *et al.* 1998; Stanford *et al.* 1998; Blakeslee *et al.* 2003; Jaffé *et al.* 2011). The universality of the CMR has been shown through many works (Visvanathan and Sandage 1977; Sandage and Visvanathan 1978a,b; Bower *et al.* 1992a,b).

The CMR parameters (slope, zero-point, and scatter) were studied at redshifts up to $z \sim 1.3$ by a number of workers (Mei *et al.* 2009 and Foltz *et al.* 2015). They found that these parameters exhibit no evolution up to this redshift limit. Cerulo *et al.* (2016) studied the evolution of the CMR at even higher redshifts. They found that, by comparing with low-redshift clusters, the CMR slope and scatter have not undergone significant evolution since $z = 1.5$. According to van Dokkum and Franx (2001), the reason for this is that the high-redshift sample does not include the bluer progenitors of the low-redshift CMR sample.

The existence of the CMR at higher redshifts may be an indication of the passive evolution of cluster elliptical galaxies proposed by the monolithic collapse scenario (Eggen *et al.* 1962). According to this scenario, elliptical galaxies are formed in a monolithic collapse at high redshift, and then evolve passively. The slope of the CMR is interpreted by Arimoto and Yoshii (1987) as a mass-metallicity effect, by adopting the supernovae-driven wind model (Larson 1974). In this model, the interstellar medium is heated by supernova explosions in the initial starburst. When the thermal energy of the gas exceeds its binding energy, a galactic wind is formed, ejecting the gas from the galaxies. More massive galaxies, due to their deeper potential well, can retain their gas for longer times than less massive ones, and thus reach higher stellar metallicities. This makes more massive (brighter) galaxies along the red sequence become redder. This mass-metallicity relation

has been adopted by Kauffman and Charlot (1998), using a hierarchical merging model. They use semi-analytic techniques to examine this relation through forming of massive elliptical galaxies from the merger of massive disk galaxies in a hierarchical fashion.

Worthy *et al.* (1996) shows that the CMR of local elliptical galaxies may also be due to an increase in mean stellar age with luminosity. However, Kodama and Arimoto (1997) show that the existence of the CMR at higher redshifts does not support the age hypothesis. They use the observational color-magnitude diagrams of E/S0 galaxies in two distant clusters Abell 2390 (z=0.228) and Abell 851 (z=0.407). They show that the bulk of stars were formed early in elliptical galaxies and that the CMR takes its origin at early times from supernovae-driven galactic winds. The age hypothesis requires a rapid evolution and disappearance of the CMR beyond certain redshift as fainter galaxies approach their formation epoch (Kodama and Arimoto 1997).

The slope of the red sequence may be used to constrain the formation epoch of elliptical galaxies within cluster cores according to Gladders *et al.* (1998). They show that the formation of at least some clusters must have been at $z > 2$. The slope is calibration-independent, so that its measurement is more reliable than measurements of color and scatter.

In this paper, we investigate the color–magnitude relations of a sample of 12 clusters, selected from Abell catalog (Abell *et al.* 1989), within the redshift range ($0.02 \lesssim z \lesssim 0.10$). All clusters have X-ray luminosities greater than 10^{44} erg s^{-1}. In each cluster, we consider only member galaxies within the inner 0.75 Mpc. In Section 2, we describe our sample and photometric data in detail, and the analysis and discussion of the color–magnitude relations of our sample clusters are given in Section 3. Our conclusions are outlined in Section 4. Throughout this work, we use ΛCDM cosmology ($\Omega_M = 0.27$, $\Omega_\Lambda = 0.73$, $H_0 = 73$ km s^{-1} Mpc^{-1}).

2. Sample and data

Our sample consists of 12 nearby clusters, selected from Abell catalog (Abell *et al.* 1989),within the redshift range ($0.02 \lesssim z \lesssim 0.10$). They all have X-ray luminosities above 10^{44} erg s^{-1}, to ensure having high mass environments. Table 1 shows the general information regarding the sample clusters. All the photometric data are taken from the Sloan Digital Sky Survey – Data Release 9 (Ahn *et al.* 2012). We use g-band and r-band model magnitudes for calculating colors, which are then plotted against r-band Petrosian magnitudes. All these magnitudes are corrected for foreground galactic extinction, and also for K-correction to obtain the rest-frame color–magnitude diagrams.

In order to confirm cluster membership, we select only galaxies with known redshifts from SDSS-DR9 database. For data completion, we also use the NASA/IPAC Extragalactic Database (NED), and the literature (Agulli *et al.* 2016, for A85 and Berrington *et al.* 2002, for A2256) to determine member galaxies having

Table 1. The sample data.

	Equ. J2000[a]			
Cluster	R.A.	Dec.	Redshift[a]	$L_x^{(b)}$ 10^{-44} erg/s
A1656	12 59 48.7	+27 58 50	0.0231	7.77
A2199	16 28 38.0	+39 32 55	0.0302	4.09
A2063	15 23 01.8	+08 38 22	0.0349	2.20
A2052	15 16 44.0	+07 01 07	0.0355	2.52
A0119	00 56 18.3	−01 13 00	0.0442	3.30
A0085	00 41 50.1	−09 18 09	0.0551	9.41
A2256	17 03 43.5	+78 43 03	0.0581	7.40
A1795	13 48 53.0	+26 35 44	0.0625	10.26
A1767	13 36 06.1	+59 12 28	0.0703	2.43
A2065	15 22 42.6	+27 43 21	0.0726	5.55
A2255	17 12 31.0	+64 05 33	0.0806	5.54
A2142	15 58 20.6	+27 13 37	0.0909	21.24

[a] These data have been taken from the NED database. [b] This is the total X-ray luminosity in 0.1–2.4 keV band, taken from the BAX database.

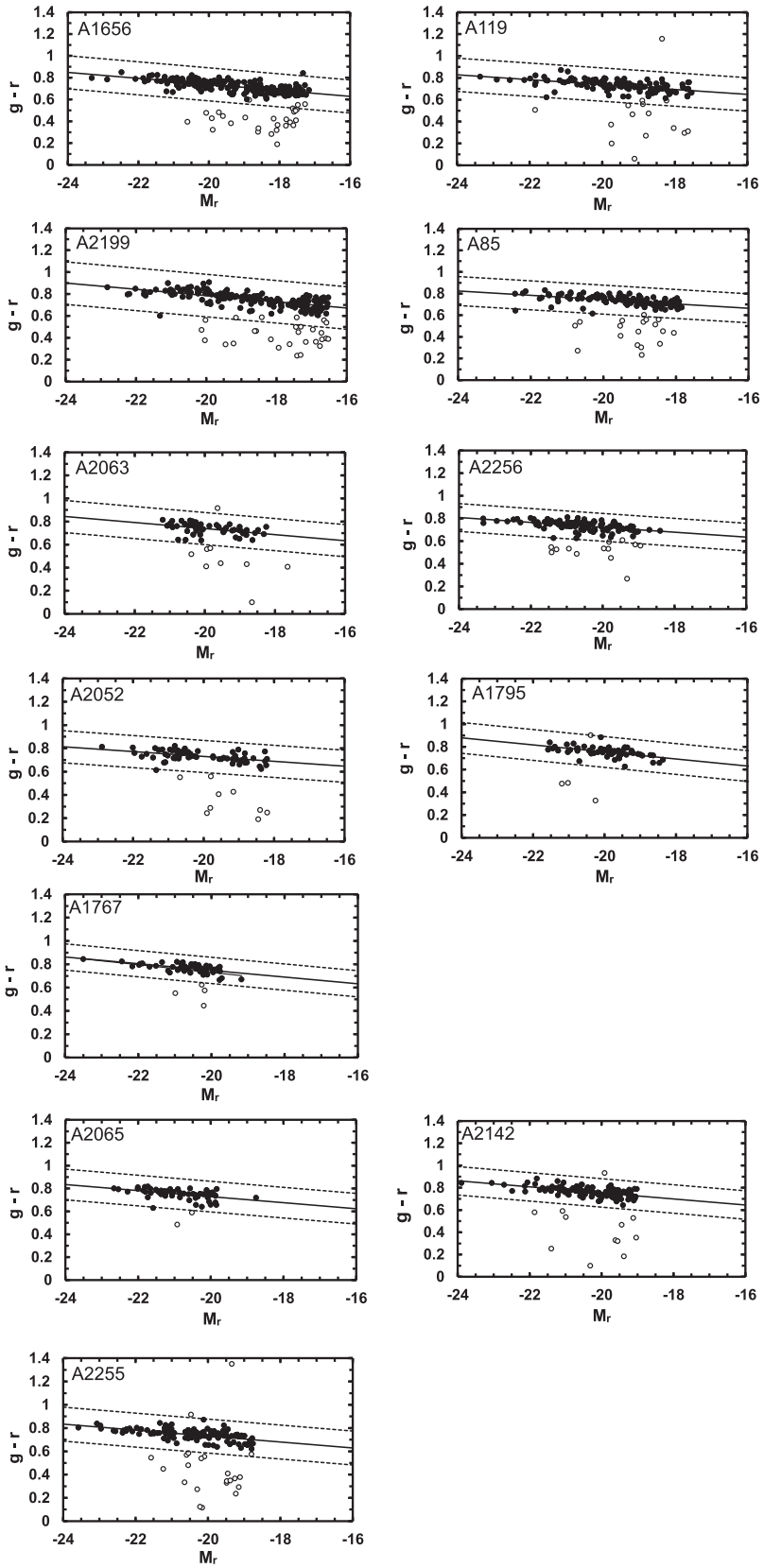

Figure 1. The rest-frame color–magnitude diagrams $(g-r)/M_r$ of our cluster sample. The solid line denotes the best-fit line, and the dashed lines are the $\pm 3\sigma$ limits used for determining the red sequence. Filled circles denote red-sequence galaxies, while open circles denote others members.

known redshifts (or radial velocities). In this case a position matching with SDSS-DR9 is achieved to extract the required photometric data. To eliminate foreground and background galaxies, and retain only members, we select those galaxies whose radial velocities lie within $\pm 3\sigma$ (velocity dispersion) from the mean radial velocity of the cluster. This is because cluster members, due to gravitation, move at relatively adjacent velocities. Since red-sequence galaxies are, in general, early-type galaxies inhabiting cluster cores, we consider only those members which lie within a projected radius of 0.75 Mpc, following Lucia *et al.* (2007). This corresponds to about $0.55R_{500}$ for our low-redshift sample, where the cluster virial radius R_{500} is the radius where the mass density is about 500 times the critical density at the cluster's redshift (Rabitz *et al.* 2017).

3. Analysis and discussion

Rest-frame color–magnitude diagrams for the sample clusters are constructed, using photometric data retrieved from SDSS-DR9 database. For this reason, we obtain the absolute Petrosian r-band magnitudes from their corresponding apparent ones, using the equation

$$M_{\mathrm{r}} = m_{\mathrm{r}} - 5\log_{10}(D_L) - 25 - K(z) - A_\lambda/\sin(b)$$

where D_L is the luminosity distance, $K(z)$ is the K-correction, A_λ is the galactic foreground extinction, given by Schlafly and Finkbeiner (2011), and b is the galactic latitude. We utilize a web-based service (Chilingarian *et al.* 2010; Chilingarian & Zolotukhin 2012) for computing K-corrections by approximating them as two-dimensional low-order polynomials of redshift and one observed color.

For a better estimation, and a less contamination of the CMRs, we take only the member galaxies with apparent r-band magnitudes less than 19 and (g – r) colors greater than 0.6, as adopted by Agulli *et al.* (2016). The best-fit line is obtained by adopting a robust 3-σ clipping method to remove the outliers, where σ is the dispersion about the best-fit line. Figure 1 displays the rest-frame (g – r)/M_r color–magnitude diagrams of our sample clusters. The solid line in each panel refers to the best-fit line, and the dashed lines are the $\pm 3\sigma$ limits used to determine the red sequence, following De Lucia *et al.* (2004). The results are summarized in Table 2.

A common feature of all CMRs, seen in Fig. 1, is their tightness. The very small dispersion in the color of all clusters from the best-fitting CMR, as noted in Table 2, demonstrates a high degree of uniformity in the star formation history of their cores (Bower *et al.* 1992a). Also, this scatter, as shown in Table 2, reveals almost no evolution with redshift, having a mean value of ~ 0.047. Another feature of the CMRs in Fig. 1 is the observed change in galaxy color along the red sequence of each cluster in such a way that fainter galaxies become bluer. This is due to either a change in the mean stellar metallicities of cluster galaxies or a decrease in age towards fainter galaxies, according to Kodama and Arimoto (1997).

The evolution of the rest-frame CMR slopes with redshift is displayed in Fig. 2. The very slight steepening of this slope with redshift, seen in the figure [best-fitting $\Delta(\text{slope})/\Delta z \sim -0.025$, assuming a linear trend, as

Table 2. Summary of results.

		CMR parameters		
Cluster	Redshift	Slope	Zero-point*	Scatter
A1656	0.0231	-0.0276 ± 0.0018	0.7377 ± 0.0502	0.051
A2199	0.0302	-0.0285 ± 0.0024	0.7862 ± 0.0655	0.065
A2063	0.0349	-0.0263 ± 0.0071	0.7389 ± 0.1996	0.046
A2052	0.0355	-0.0209 ± 0.0045	0.7304 ± 0.1271	0.046
A0119	0.0442	-0.0224 ± 0.0031	0.7384 ± 0.0863	0.051
A0085	0.0551	-0.0200 ± 0.0031	0.7442 ± 0.0870	0.044
A 2256	0.0581	-0.0216 ± 0.0035	0.7222 ± 0.1008	0.041
A1795	0.0625	-0.0310 ± 0.0062	0.7552 ± 0.1757	0.045
A1767	0.0703	-0.0287 ± 0.0050	0.7476 ± 0.1443	0.037
A2065	0.0726	-0.0264 ± 0.0065	0.7290 ± 0.1882	0.045
A2255	0.0806	-0.0256 ± 0.0035	0.7313 ± 0.1005	0.049
A 2142	0.0909	-0.0272 ± 0.0034	0.7537 ± 0.0972	0.043

* The zero-point has been measured at the absolute magnitude $M_r = -20$.

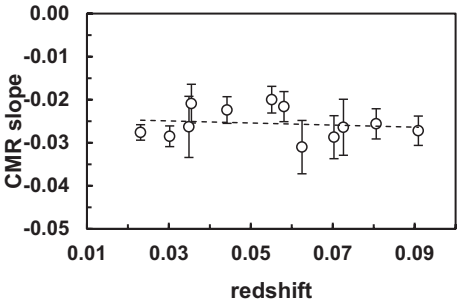

Figure 2. The evolution of the rest-frame CMR slope with redshift. The dashed line denotes the best-fit line.

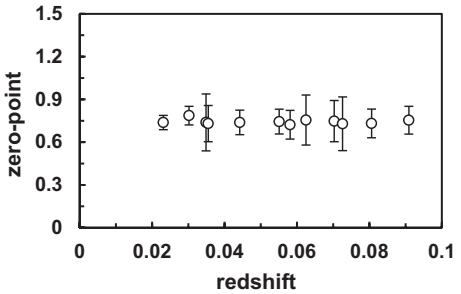

Figure 3. The evolution of the rest-frame CMR zero-point with redshift. The zero-point has been measured at the absolute magnitude $M_r = -20$.

adopted by Hao *et al.* (2009)], indicates that almost no contribution is noted from an age or a metallicity evolution. Thus, during the look-back time of $z \sim 0.1$ no significant star formation activity has occurred. This means that, within the redshift range considered in this work, all galaxies on the red sequence are passively evolving, early-type (E/S0) members.

Figure 3 shows the evolution of the zero-point of the CMR. Its values have been measured at the rest-frame absolute magnitude $M_r = -20$. As we see, no significant evolution is revealed by this parameter within the redshift range considered in this work. This may be due to similar stellar formation histories of these clusters.

4. Conclusions

We study the CMRs of 12 clusters selected from Abell catalogue within the redshift range ($0.02 \lesssim z \lesssim 0.10$) using SDSS-DR9 photometric data.For these low-redshift clusters, we observe that the basic parameters of the CMR (slope, zero-point, and scatter) do not exhibit significant evolution. This shows that these red sequence galaxies are passively evolving with no star formation activity. The importance of such results is that it may be considered as a reference for studying the characteristics of the CMR at higher redshifts, in order to gain knowledge about the evolutionary stages of galaxies within clusters.

Acknowledgements

Funding for SDSS-III has been provided by the Alfred P. Sloan Foundation, the Participating Institutions, the National Science Foundation, and the U.S. Department of Energy Office of Science. The SDSS-III web site is http://www.sdss3.org/. SDSS-III is managed by the Astrophysical Research Consortium for the Participating Institutions of the SDSS-III Collaboration including the University of Arizona, the Brazilian Participation Group, Brookhaven National Laboratory, Carnegie Mellon University, University of Florida, the French Participation Group, the German Participation Group, Harvard University, the Instituto de Astrofisica de Canarias, the Michigan State/Notre Dame/JINA Participation Group, Johns Hopkins University, Lawrence Berkeley National Laboratory, Max Planck Institute for Astrophysics, Max Planck Institute for Extraterrestrial Physics, New Mexico State University, New York University, Ohio State University, Pennsylvania State University, University of Portsmouth, Princeton University, the Spanish Participation Group, University of Tokyo, University of Utah, Vanderbilt University, University of Virginia, University of Washington, and Yale University. This research has made use of the NASA/IPAC Extragalactic Database (NED) which is operated by the Jet Propulsion Laboratory, California Institute of Technology, under contract with the National Aeronautics and Space Administration. The research has also made use of "Aladin Sky Atlas" developed at CDS, Strasbourg Observatory, France (Bonnarel *et al.* 2000 and Boch and Fernique 2014). It has also made use of the TOPCAT software (Taylor 2005). This research has made use of the X-Rays Clusters Database (BAX) which is operated by the Laboratoire d'Astrophysique de Tarbes-Taulouse (LATT), under contract with the Centre National d'Etude Spatiales (CNES).

References

Abell G. O., Corwin H. G., Jr., Olowin R. P. 1989, ApJS, 70, 1

Agulli I. *et al.*, 2016, MNRAS, 458, 1590

Ahn C. P. *et al.*, 2012, ApJS, 203, 21

Arimoto N. Yoshii Y., 1987, A&A, 173, 23

Baum W. A., 1959, PASP, 71, 106
Berrington R. C., Lugger P. M., Cohn H. N., 2002, AJ, 123, 2261
Blakeslee, J. P. *et al.*, 2003, ApJL, 596, L143
Boch T., Fernique P. 2014, ASP Conference Series, Volume 485
Bonnarel F. *et al.*, 2000, A&AS, 143,33
Bower R. G., Lucey J. R., Ellis R. S., 1992a, MNRAS, 254, 589
Bower R. G., Lucey J. R., Ellis R. S., 1992b, MNRAS, 254, 601
Carlberg R. G., 1984, ApJ, 286, 416
Cerulo P. *et al.*, 2016, MNRAS, 457, 2209
Chilingarian I. V., Melchior A., Zolotukhin I. Y., 2010, MNRAS, 405, 1409
Chilingarian I. V. Zolotukhin I. Y., 2012, MNRAS, 419, 1727
De Lucia G. *et al.*, 2004, ApJ, 610, L77
De Lucia G. *et al.*, 2007, MNRAS, 374, 809.
Eggen O. J., Lynden-Bell D., Sandage A. R., 1962, ApJ, 136, 748
Ellis R. S., Smail I., Dressler A., Cough W. J., 1997, ApJ, 483, 582
Foltz R. *et al.*, 2015, ApJ, 812, 138
Gladders M. D., López-Cruz O., Yee H. K. C., Kodama T. 1998, ApJ, 501, 571
Hao J. *et al.*, 2009, ApJ, 702, 745
Jaffé Y. L. *et al.*, 2011, MNRAS, 410, 280
Kauffman G. Charlot S., 1998, MNRAS, 294, 705
Kodama T. Arimoto N., 1997, A&A, 320, 41
Larson R. B., 1974, MNRAS, 169, 229
Mei S. *et al.*, 2009, ApJ, 690, 42
Rabitz A. *et al.*, 2017, A&A, 597, A24
Sandage A. Visvanathan N., 1978a, ApJ, 223, 707
Sandage A. Visvanathan N., 1978b, ApJ, 225, 742
Schlafly E. F. Finkbeiner D. P., 2011, ApJ, 737, 103
Stanford S. A., Eisenhardt P. R., Dickinson M., 1998, ApJ, 492, 461
Taylor M. B. 2005, ASP Conference Series, Volume 347, p. 29
van Dokkum P. G. *et al.*, 1998, ApJ, 500, 714
van Dokkum P. G. Franx M., 2001, ApJ, 553, 90
Visvanathan N. Sandage A., 1977, ApJ, 216, 214
Worthy G., Trager S. C., Faber S. M. 1996, ASP Conference Series, Volume 86, p. 203